Electronic Supplementary Material (ESI) for Inorganic Chemistry Frontiers.

Supporting information for:

Self-assembled manganese acetate@tin dioxide colloidal quantum dots as electron transport layer for effcient and stable perovskite solar cells

Yutao Li[1], Chenyu Zhao[1], Lexin Wang[1], Lin Fan[1, 2], Maobin Wei[1, 2], Huilian Liu[1, 2], Xiaoyan Liu[1, 2], Jinghai Yang[1, 2]*, Fengyou Wang[1, 2]*, Lili Yang[1, 2]*

1. Key Laboratory of Functional Materials Physics and Chemistry of the Ministry of Education, Jilin Normal University, Changchun 130103, China
2. National Demonstration Center for Experimental Physics Education, Jilin Normal University, Siping 136000, China

Experimental section & Materials

Supplementary note 1

Materials: $Mn(Ac)_2$ was purchased from Aladdin. Lead iodide (PbI_2), formamidineiodide (FAI), lead bromide ($PbBr_2$), Cesium iodide (CsI), Methylammonium chloride (MACl), methylammonium bromide (MABr), 4-tert-butypyridine and lithium bis (trifluoromethanesulfonyl) imide (Li-TFSI), tris(2-(1H-pyrazol-1-yl)-4-tertbutylpyridine)-cobalt(III)tris(bis(trifluoromethylsulfonyl)imide) (FK209), tert-butylpyridine (TBP), SnO_2 aqueous colloidal dispersion (15wt%), 2,2′,7,7′-tetrakis (N,N-dip-methoxyphenylamine) and 9,9′-Spirobifluorene (Spiro-OMeTAD) were purchased from Xi'an Yuri Solar Co., Ltd. Indium Tin Oxides (ITO) glass substrates, Dimethyl sulfoxide (DMSO) and N,N-Dimethylformamide (DMF) were purchased from YOUXUAN Technology Co. Ltd. (China). Chlorobenzene (CB) were purchased from Beijing InnoChem Science & Technology Co., Ltd. All chemicals and reagents were used as received from chemical companies without any further purification.

Supplementary note 2

Characterization: The scanning electron microscope (SEM) images was taken using a Hitachi S-4800. AFM was measured by Park NX20, Korea. The transmission electron microscopy (TEM) images was taken using JEOL 2100F. The optical properties of the films were analyzed using a UV-Vis spectrophotometer (Shimadzu, UV-3600Plus, Japan). Fourier transform infrared spectroscopy (FTIR) was measured by Nicolet iS10, America. The scanning electron microscope (SEM) images was taken using a Hitachi S-4800. AFM was measured by Park NX20, Korea. The crystal structure of the SnO_2 and the perovskite samples were carried out by X-ray diffraction (XRD) (PANalytical X-ray Spectrometer Empyrean DY01660 ID206161). PL spectra were obtained using a PL microscopic spectrometer (FLS1000, China) with a 405 nm CW laser excitation source. The TRPL (FLS1000, China) was measured by using an excitation wavelength of 405nm. The main corresponding setup consisted of perovskite, and mica-flakes. The transient photovoltage spectrum (TPV) was measured by CEL-TPV2000 (CEAULIGHT, China). X-ray photoelectron spectroscopy (XPS) was used to obtain the chemical states information (measured by Escalab250Xi, Germany). *J-V* characterizations was carried out under AM 1.5 G simulated sunlight illuminations (100 mW cm^{-2}, Model 94043A, Oriel, American). Electrical impedance spectroscopy (EIS) was performed by using the electrochemical workstation (CHI660C, Chen Hua, China) with a frequency range from 1 Hz to 0.1MHz in the dark. The spectral responses were obtained from an EQE measurement system (Newport PV measurement, American).

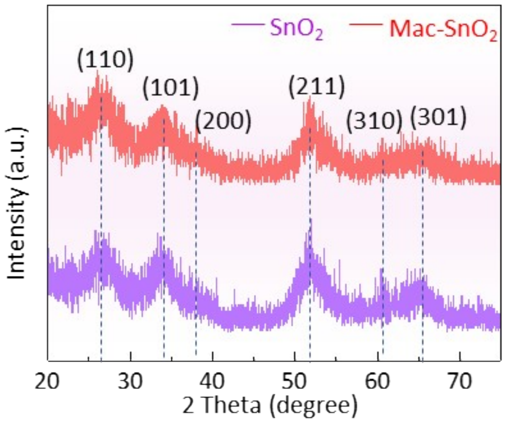

Fig. S1. XRD patterns of SnO_2 and Mac-SnO_2 films on glass substrates.

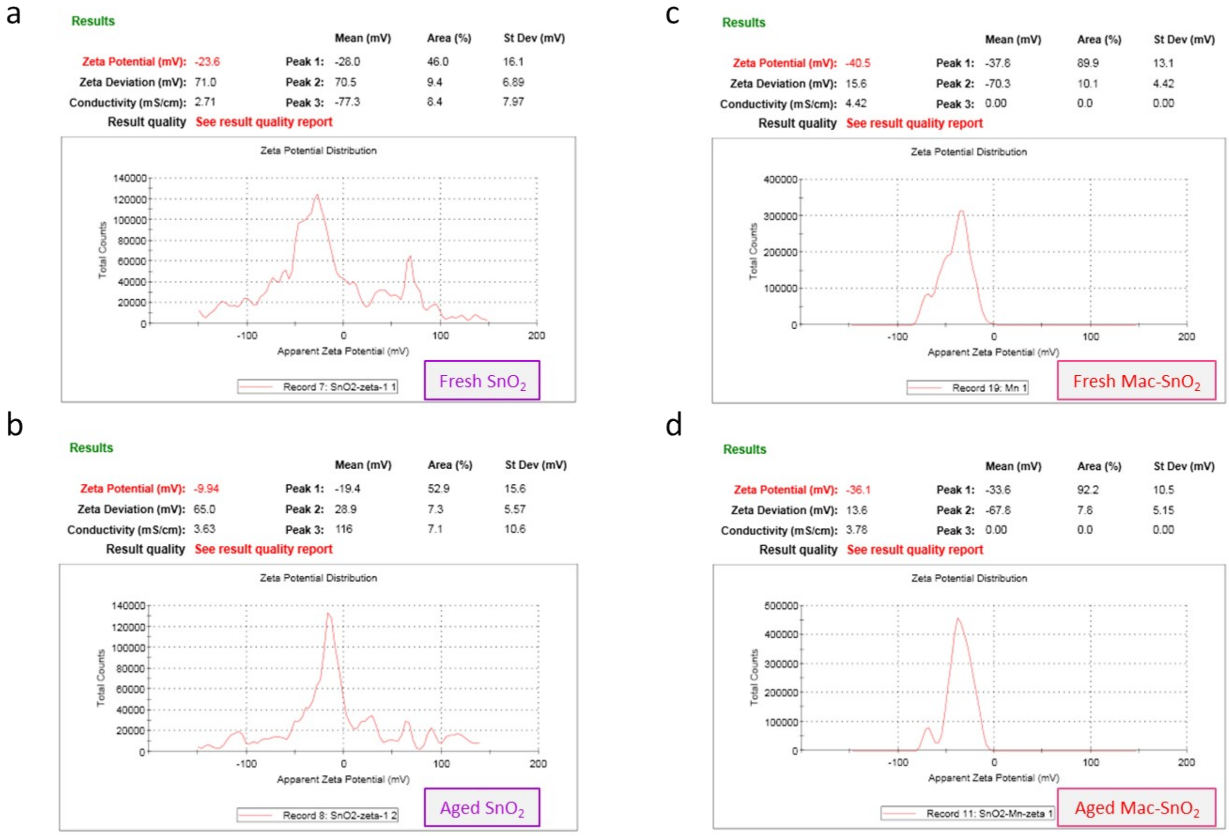

Fig. S2. Surface zeta potential of fresh (a) SnO_2 and (b) Mac-SnO_2 solutions. Surface zeta potential of 72 hours aged (c) SnO_2 and (d) Mac-SnO_2 solutions.

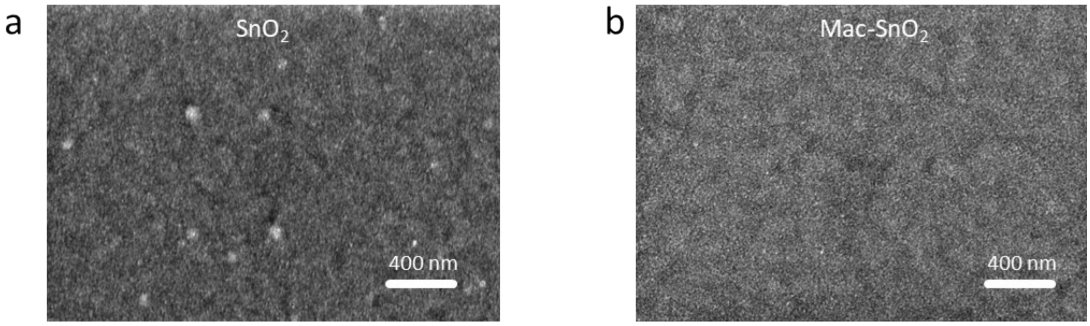

Fig. S3. The SEM images of (a) SnO_2 and (b) Mac-SnO_2 films.

Fig. S4. Photograph of the SnO_2 and Mac-SnO_2 solutions.

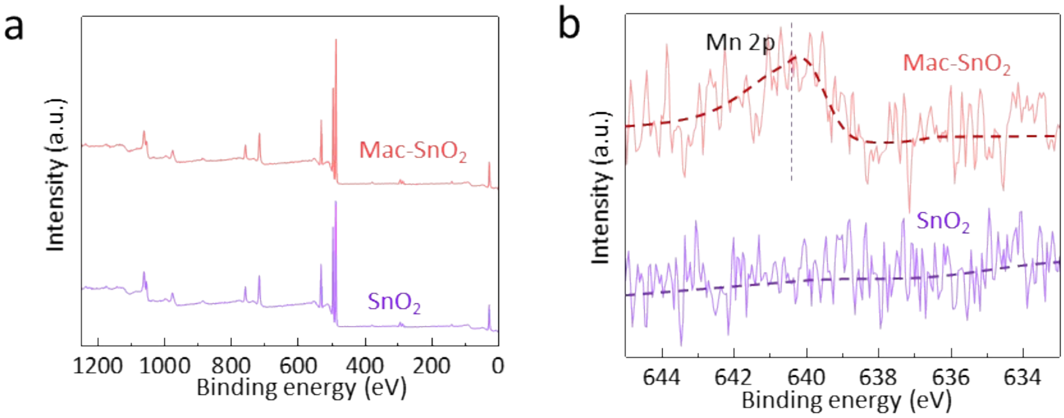

Fig. S5. XPS results of the SnO_2 and Mac-SnO_2. (a) full spectra; (b) the amplified spectra of Mn 2p signals.

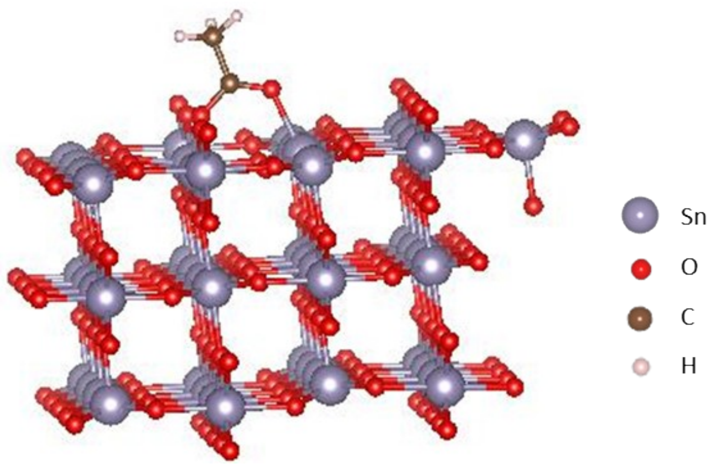

Fig. S6. Side view of the optimized SnO_2-O_v/Ac^-.

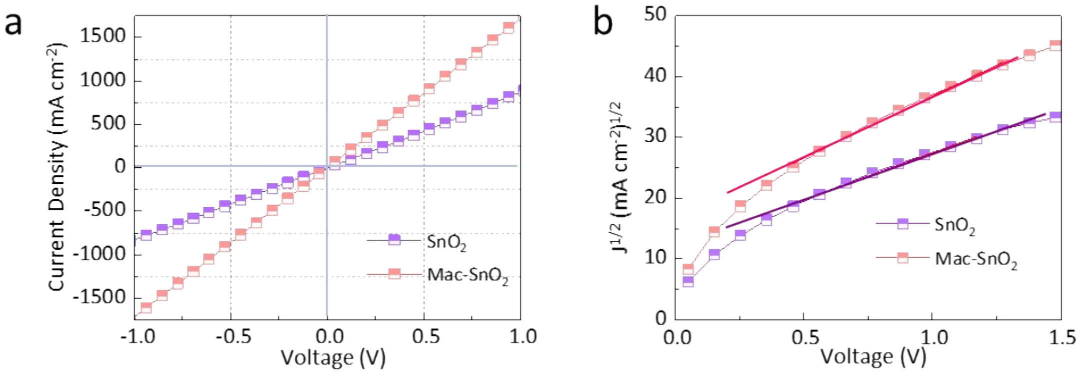

Fig. S7. The (a) conductivity and (b) electronic mobility of SnO_2 and Mac-SnO_2 films.

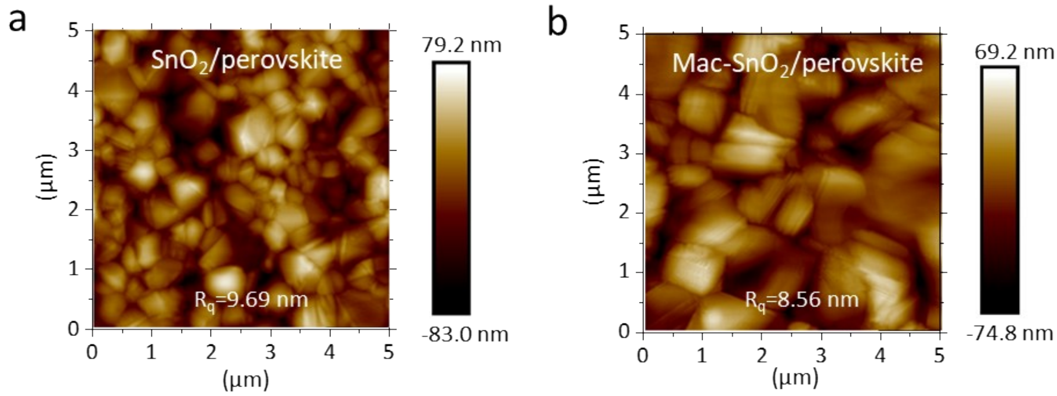

Fig. S8. AFM images of SnO_2/perovskite and Mac-SnO_2/perovskite films.

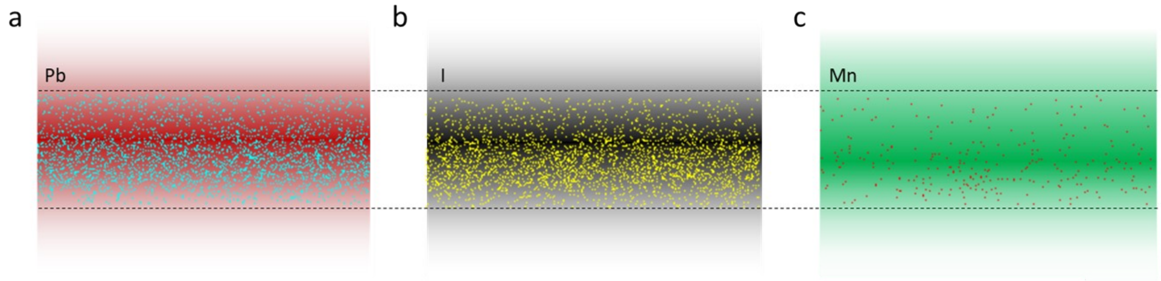

Fig. S9. The SEM element mapping analysis of (a) Pb, (b) I, and (c) Mn of the Mac-SnO_2/perovskite films.

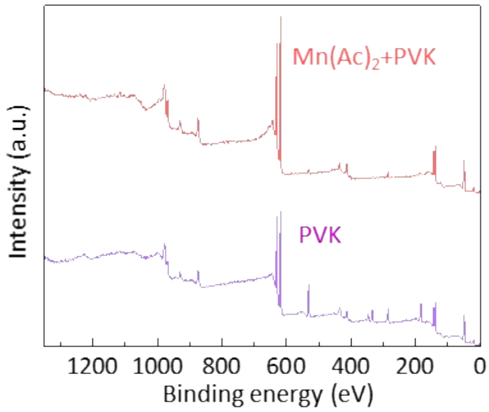

Fig. S10. XPS full spectra of the perovskite and $Mn(Ac)_2$+perovskite.

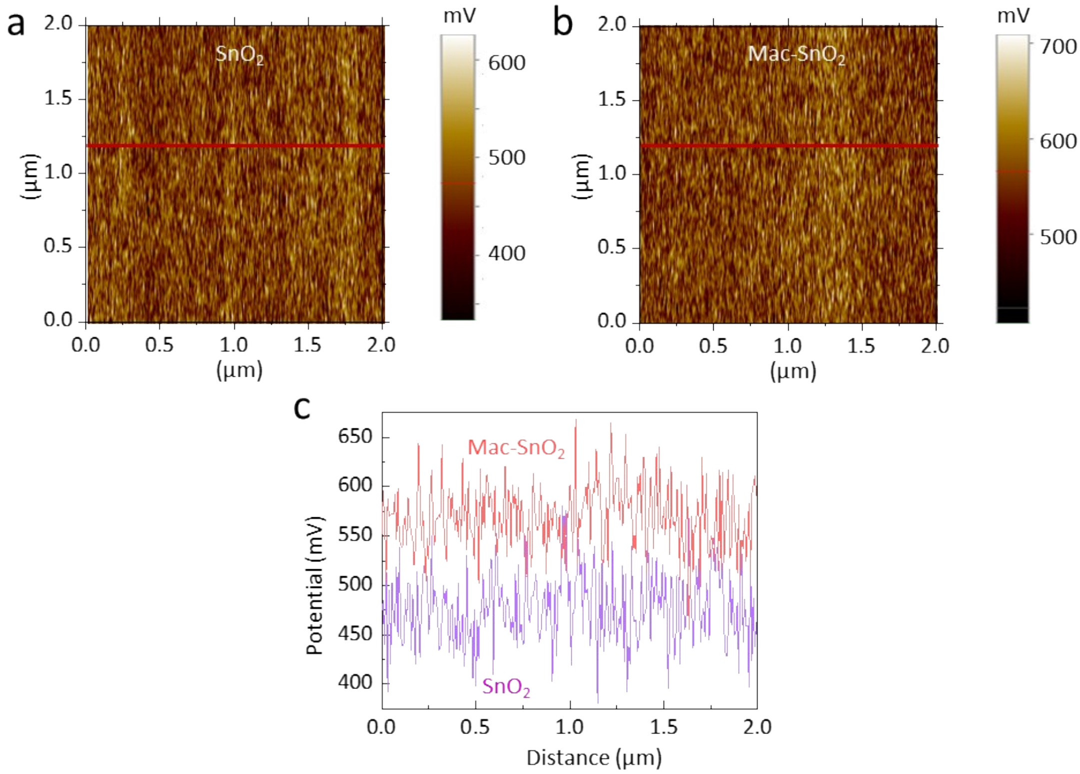

Fig. S11. KPFM images of (a) SnO_2 and (b) Mac-SnO_2 films. (c) Surface potential data of SnO_2 and Mac-SnO_2 films extracted from KPFM.

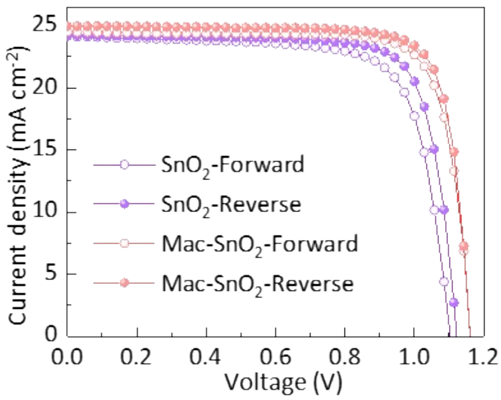

Fig. S12. *J–V* curves of the SnO_2 and Mac-SnO_2 based PSCs at forward and reverse scans.

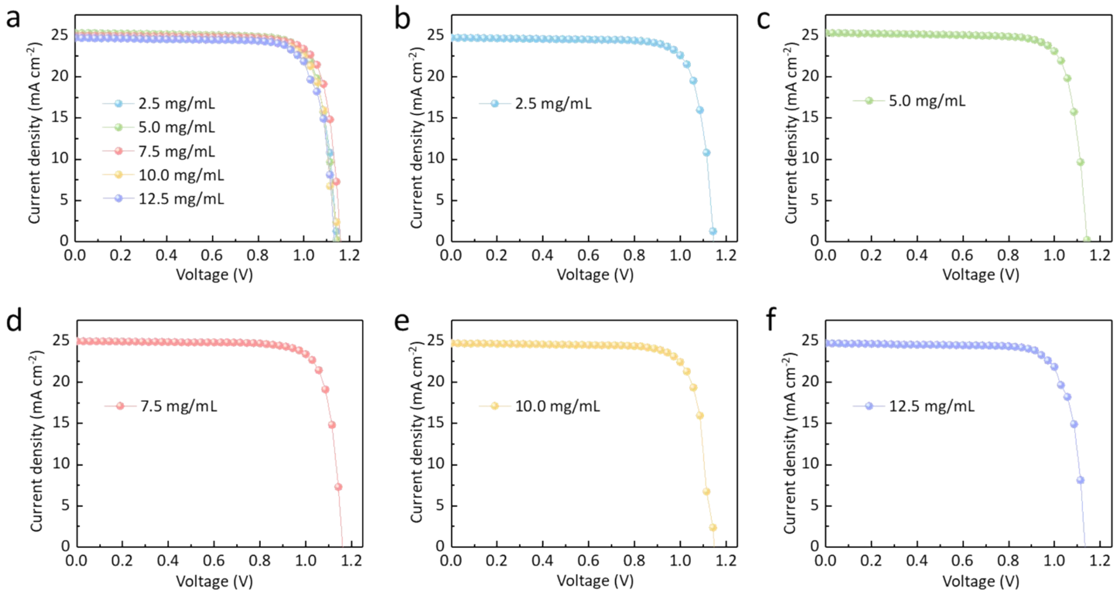

Fig. S13. *J-V* curves in reverse scan of the PSCs based on different Mac-SnO_2 concentrations.

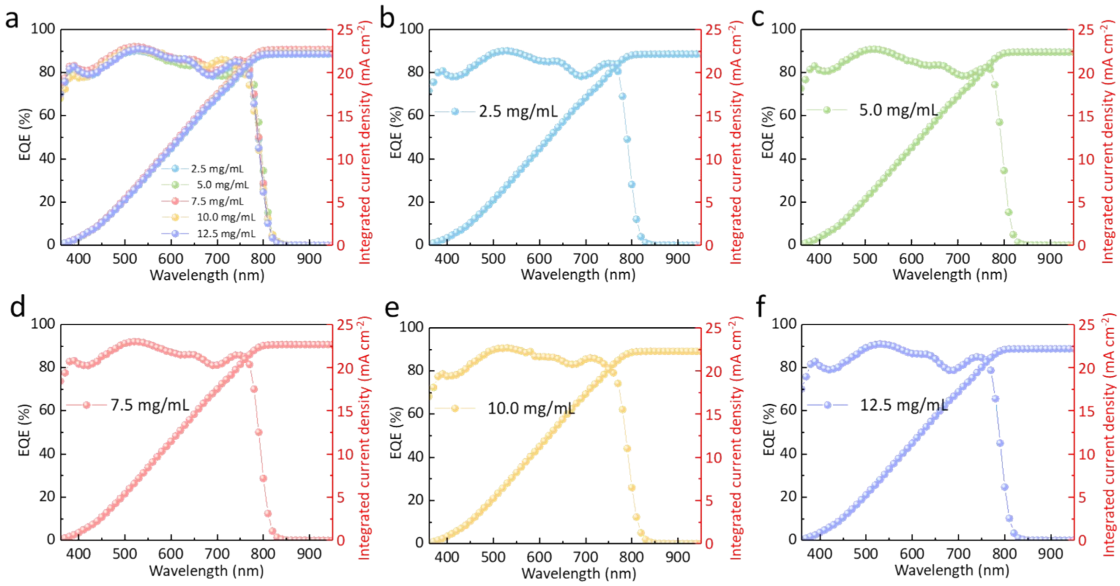

Fig. S14. EQE spectra of the PSCs based on different Mac-SnO_2 concentrations.

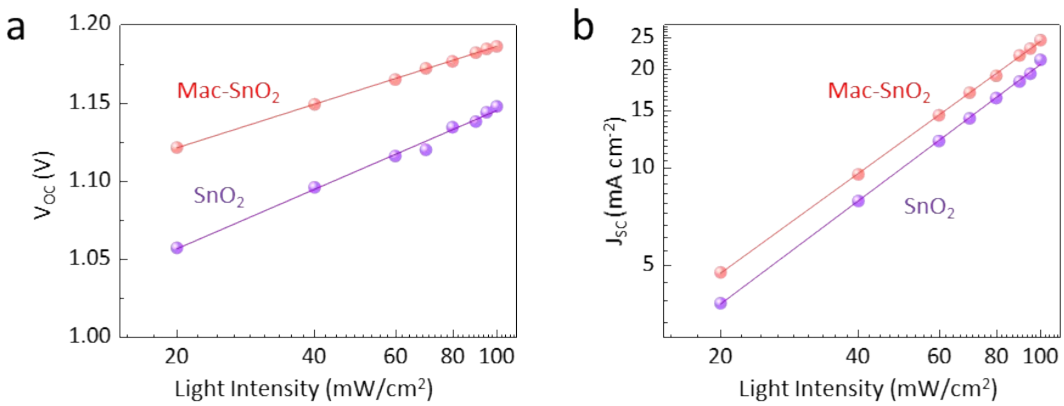

Fig. S15. (a) The dependence of V_{oc} on light intensity for SnO_2 and Mac-SnO_2 based devices. (b) The dependence of J_{sc} on light intensity for SnO_2 and Mac-SnO_2 based devices.

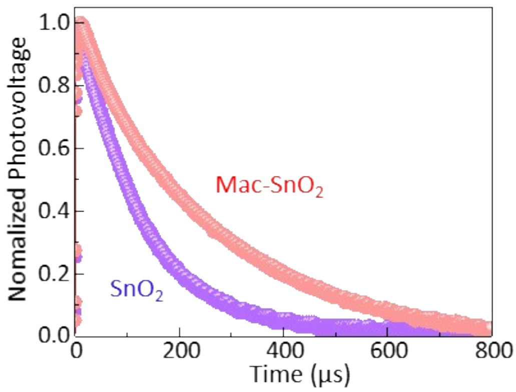

Fig. S16. TPV curves of SnO_2 and Mac-SnO_2 based devices.

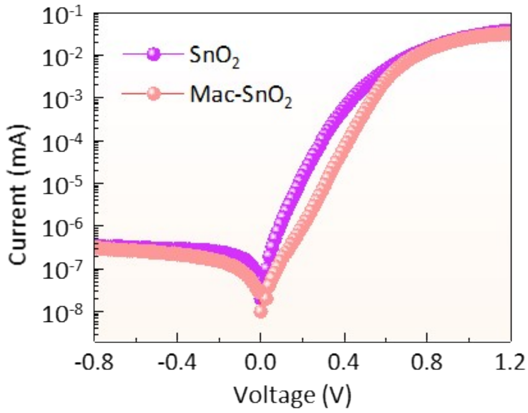

Fig. S17. Dark *I*–*V* curves of the PSCs based on SnO_2 and Mac-SnO_2 ETL.

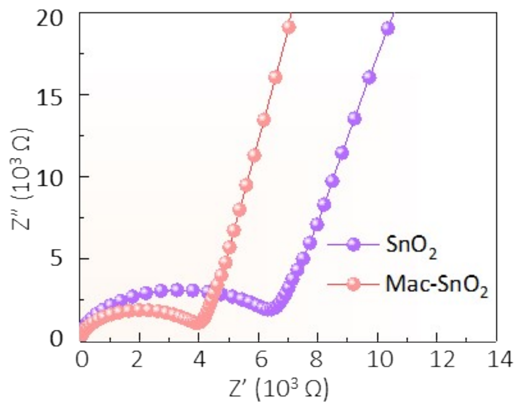

Fig. S18. Nyquist plots of the SnO_2 and Mac-SnO_2 based devices.

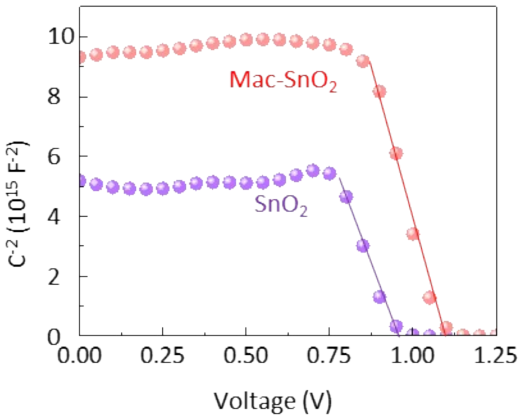

Fig. S19. Mott-Schottky plots of SnO_2 and Mac-SnO_2 based devices.

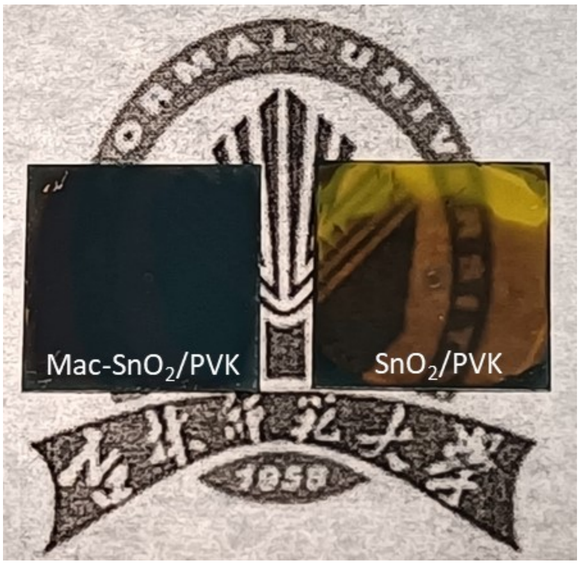

Fig. S20. Photograph of SnO_2/perovskite and Mac-SnO_2/perovskite exposed to air environment with 30%–40% humidity for 20 days.

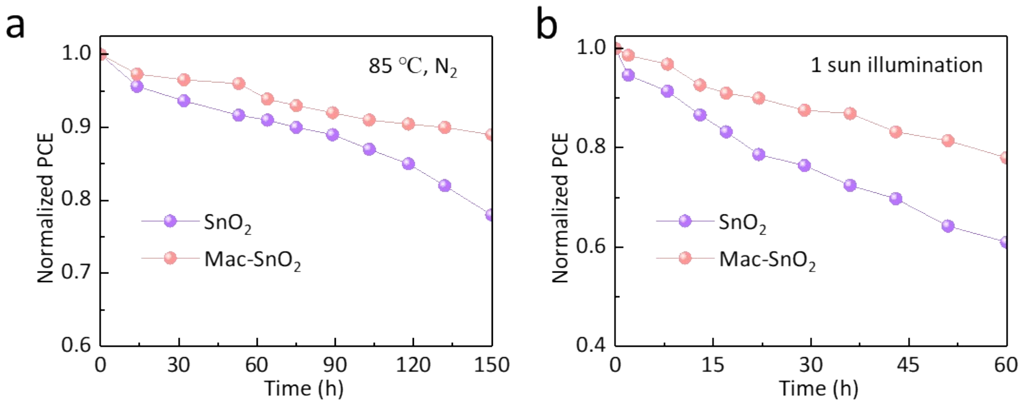

Fig. S21. Normalized *PCEs* of SnO_2 and Mac-SnO_2 based devices stored (a) at 85 °C in N_2 atmosphere and (b) under 1 sun illumination.

Table S1. Detail values of V_{oc}, J_{sc}, FF and PCE for Mac-SnO_2 based and SnO_2 based devices.

	V_{oc} (V)	J_{sc} (mA cm^{-2})	FF (%)	PCE (%)
Mac-SnO_2-Reverse	1.16	24.96	80.69	23.36
Mac-SnO_2-Forward	1.15	24.49	80.47	22.56
SnO_2-Reverse	1.12	24.25	77.66	21.11
SnO_2-Forward	1.10	24.12	74.29	19.75

Table S2. Photovoltaic parameters derived from the champion devices with different Mac-SnO_2 concentrations.

	V_{oc} (V)	J_{sc} (mA cm^{-2})	*FF* (%)	*PCE* (%)
2.5 mg/mL	1.14	24.73	79.86	22.58
5.0 mg/mL	1.14	25.32	80.00	23.08
7.5 mg/mL	1.16	24.96	80.69	23.36
10.0 mg/mL	1.14	24.72	79.38	22.44
12.5 mg/mL	1.13	24.72	78.05	21.81

Table S3. The output parameters of the SnO_2 based devices.

	V_{oc} (V)	J_{sc} (mA cm^{-2})	*FF* (%)	*PCE (%)*
1	1.09	23.93	79.04	20.64
2	1.08	24.21	77.66	20.29
3	1.09	22.71	79.74	19.82
4	1.09	22.60	78.27	19.32
5	1.08	22.65	77.44	18.91
6	1.12	22.77	79.09	20.08
7	1.11	23.20	78.47	20.21
8	1.13	23.29	77.84	20.53
9	1.12	23.68	78.14	20.79
10	1.12	23.55	77.17	20.33
11	1.13	23.01	73.98	19.22
12	1.14	22.95	79.51	20.95
13	1.12	24.25	77.66	21.11
14	1.15	21.73	79.44	19.85
15	1.15	23.00	79.49	20.98
16	1.14	22.07	76.30	19.16
17	1.16	23.37	77.58	21.07
18	1.15	22.38	80.05	20.51
19	1.13	24.56	75.72	21.01
20	1.10	23.55	78.32	20.35

Table S4. The output parameters of the Mac-SnO_2 based devices.

	V_{oc} (V)	J_{sc} (mA cm^{-2})	*FF* (%)	*PCE (%)*
1	1.13	24.10	78.20	21.33
2	1.16	22.44	80.73	21.06
3	1.09	23.91	82.08	21.34
4	1.16	24.96	80.69	23.36
5	1.12	24.80	81.32	22.66
6	1.17	24.05	76.30	21.53
7	1.14	24.81	75.05	21.25
8	1.16	24.10	77.30	21.65
9	1.14	25.31	79.73	23.01
10	1.15	24.50	79.78	22.55
11	1.15	24.64	79.01	22.34
12	1.15	22.24	80.77	21.56
13	1.12	24.06	80.12	21.65
14	1.15	23.37	80.33	21.52
15	1.14	25.33	79.98	23.05
16	1.13	24.40	78.86	21.83
17	1.17	23.24	80.08	21.68
18	1.12	24.66	80.63	22.25
19	1.16	23.37	79.37	21.56
20	1.13	24.24	77.99	21.43